

# Sustainable Synthesis of MXenes

Subjects: [Materials Science, Ceramics](#) | [Chemistry, Applied](#) | [Nanoscience & Nanotechnology](#)

Contributor: Tahta Amrillah , Che Azurahanim Che Abdullah , Angga Hermawan , Fitri Nur Indah Sari , Vani Novita Alvani

MXenes provide a major drawback involving environmentally harmful and toxic substances for its general fabrication in large-scale production and employing a high-temperature solid-state reaction followed by selective etching. Meanwhile, how MXenes are synthesized is essential in directing their end uses. Therefore, making strategic approaches to synthesize greener, safer, more sustainable, and more environmentally friendly MXenes is imperative to commercialize at a competitive price.

MXenes

green synthesis

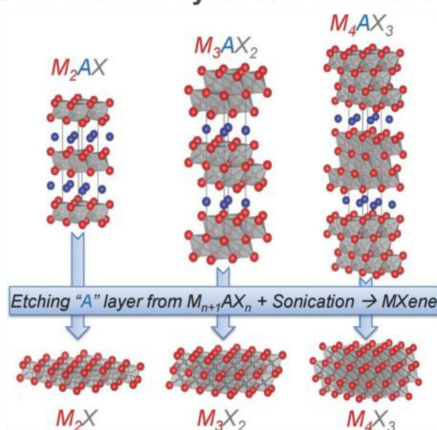
2D materials

sustainable

## 1. Introduction

MXenes are a new family of two-dimensional (2D) materials constructed of surface-modified carbide, nitride, and carbonitride. Their structures may vary depending on their chemical composition. Having a general chemical formula of  $M_{n+1}X_nT_x$  ( $n = 1, 2, 3$ , and  $4$ ), MXenes are composed of layers of early transition metals ( $M$ ) which are inserted with  $n$  layers of carbon or nitrogen ( $X$ ) and terminated with surface functional groups ( $T_x = -O, -OH$ , and  $-F$ ) [1][2]. Like other 2D materials, MXenes are conventionally synthesized by exfoliating their initial 3D precursors, namely the MAX phases, which are ternary carbides or nitrides with the general formula of  $M_{n+1}AX_n$  [1][2]. In the MAX phase, as shown in **Figure 1a**, the  $M-X$  bonds are stronger than the  $M-A$  bonds. Here, the  $A$  layers are chemically more active than the  $M-X$  layers are; thus, the  $A$  layers are easily removed by etching, mostly by using a strong acid such as hydrofluoric acid (HF) to obtain the  $M_{n+1}X_n$  layers that are typically terminated by fluorine ( $-F$ ), hydroxide ( $-OH$ ) and oxygen ( $-O$ ) groups due to their high surface energy [2].

(a) Conventional synthesis of MXenes



(b) Synthesis

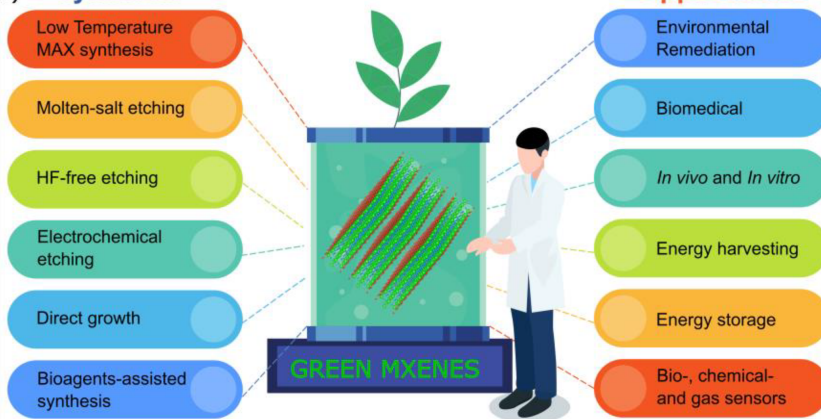


**Figure 1. (a).** Crystal structure transformation of MAX phase and their conventional exfoliation into MXenes. Adopted from reference [3]. **(b)** Green route to synthesize MXenes and their potential applications.

Recently, MXenes have received paramount attention for their broad utility, e.g., optics and electronics, energy storage and conversion, environment and catalysis, biotechnology, and medicine [1]. MXenes exhibit biological properties associated with their carbon and/or nitrogen content, and the inertness of the transition metals has been called into question. Among the methods, a straightforward one to make MXenes more feasible, particularly for biotechnology, environmental, and energy-related applications, is to modify their composition and fabricate them through the use of green synthesis technology, as illustrated in **Figure 1b** [4]. Green synthesis is defined as a clean, safe, cost-effective, and environmentally friendly process of preparing micro- or nanostructured materials. Green synthesis is mainly used to minimize the toxic synthesis agents and employ an environmentally benign process [5][6][7]. Generally, microorganisms such as bacteria, yeast, fungi, algal species, and certain plants act as substrates for the green synthesis of nanomaterials [8]. In this route, the MXenes are non-toxic and have more excellent biocompatibility than the MXenes synthesized from conventional ways that use any hydrofluoric acid (HF)-containing HF-forming chemicals do. These HF chemicals may leak into groundwater resources and endanger aquatic life and humans by polluting the drinking water if the waste solutions are not adequately handled. Thus, studies examining simple, economical, and environmentally friendly ways to mitigate their potential toxicity are highly desired [9]. The green technology of MXenes is also predicted to be a cheaper, simpler, and energy-saving alternative to conventional chemical and physical methods, significantly impacting the realization of the MXenes' uses [4][5][6].

Due to increasing research trends, green synthesis is now finding its pathway from the laboratory to commercial applications, but it still faces significant challenges. Thus far, no effective green synthesis protocol has been developed for MXenes. A more time-efficient, cost-competitive, and environmentally friendly fabrication of MXenes and MXene-based nanomaterials that allow the surface engineering of the nanostructures to be conducted for specific applications will be deemed useful. To this end, developing a viable green synthetic strategy can increase the MXenes' versatility for various medical explorations related to treatment and diagnostic approaches, environmental applications, energy storage and conversion devices, and others. A viable strategy can be made by matching key specific properties to satisfy an appropriate utilization. The terminated groups influence the surface chemistry of the MXenes, i.e., F-functionalized MXenes are unsuitable for electrode materials in energy storage and catalysis systems because the F atom decreases their electrical conductivity. MXene synthesis requires modern protocols that are both efficient and feasible, including the use of a low-boiling solvent [10], low-energy processes through physical synthesis [11], low-temperature MAX preparation, and the possible utilization of biological substances, which were previously successfully used in the fabrication of other 2D materials such as graphene [12][13]. A recent fabrication and viable strategy for green MXenes can be achieved by manipulating the MXene's diversity and green chemistry. These current green strategies include fabricating MXenes with milder etchants than HF for exfoliation, milder fluorine salts, and without fluoride [14][15]. Another approach is to use a hydrothermal method to synthesize large quantities of 2D MXene components without using toxic HF vapor, and combining Baeyer's process with alkali-induced hydrothermal technology results in multi-layered  $\text{Ti}_3\text{C}_2\text{T}_x$

production [16]. Additionally, the MXenes can be synthesized via chemical vapor deposition and salt template or molten salt syntheses.

## 2. Synthesis of MXenes

### 2.1. Conventional Synthesis of MXenes

The lengthy process for the synthesis of MXenes begins with the preparation of bulk MAX phases as a starting material, as shown in **Figure 2a**. The MAX phases refer to layered polycrystalline of ternary carbides and nitrides with the general formula of  $M_{n+1}AX_n$  ( $M$  = early transition metal,  $A$  = group III or IVA, and  $X$  = either carbon and/or nitrogen). They have an edge-sharing feature with a distorted  $M_6X$  octahedra structure interlayered by group A elements. The MAX phases were discovered in the early 1960s [17], and they were successfully prepared with the formula of  $M_2AC$  ( $Zr_2TiC$ ,  $Zr_2PbC$ ,  $Hf_2TiC$ , and  $Hf_2PbC$ ), which was called the H phase. To date, there are more than 200 MAX possible compositions, having been mostly discovered by the use of theoretical calculations. However, only a few MAX phases have been successfully synthesized due to their thermodynamic instability. The microstructure of the MAX phase ( $Ti_3AlC_2$ ) is visually shown in **Figure 2b**, and after HF etching (**Figure 2c**), it transforms into a  $Ti_3C_2$  MXene nanosheet (**Figure 2d**).

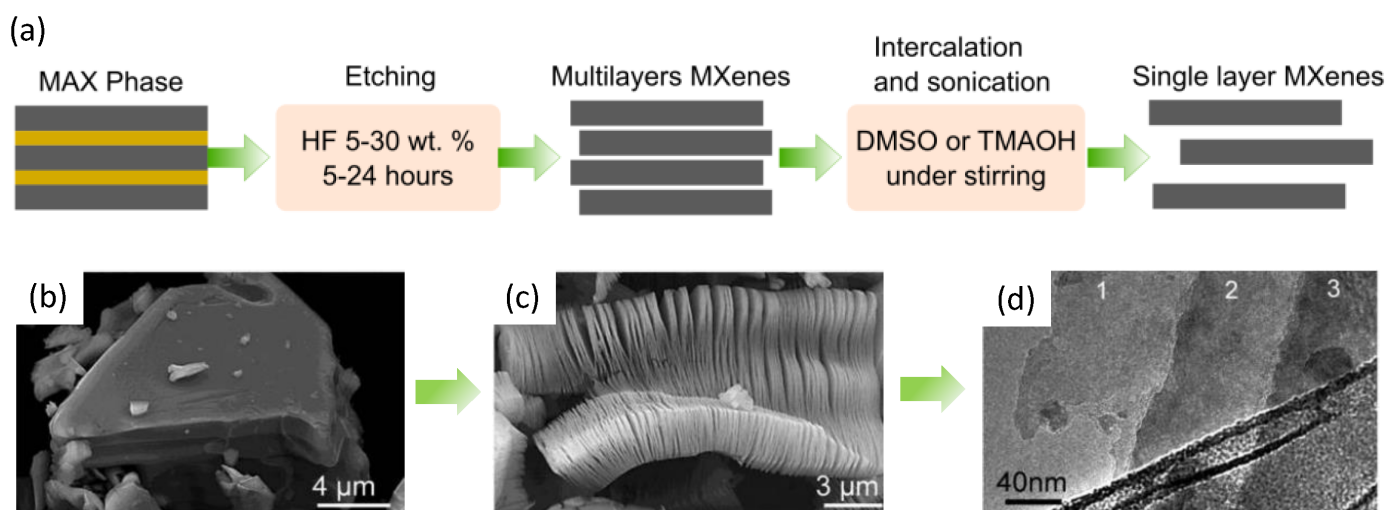


**Figure 2.** (a) General synthesis steps to produce single-layered MXenes. (b) Microstructure of MAX phase of  $Ti_3AlC_2$  particle before treatment. (c)  $Ti_3AlC_2$  after HF treatment and (d)  $Ti_3C_2$  layers formed after HF treatment of  $Ti_3AlC_2$  (a single sheet (monolayer) is the most transparent part of the sample). Adopted from reference with permission [18].

The  $M_{n+1}AX_n$  ( $n = 1$  and  $2$ ),  $Ti_2AlC$ , and  $Ti_3AlC_2$  are thermodynamically stable, and thus, they can be prepared in various temperatures. Meanwhile, in the  $Cr_{n+1}AlC_n$  and  $Ti_{n+1}SiC_n$  systems, only  $Cr_2AlC$  and  $Ti_3SiC_2$  possess thermodynamical stability. The MAX phases are generally synthesized by solid-state reactions from their respective elements at high temperatures ranging from 1200 °C to 1800 °C, depending on their compositions. The solid-state reactions should be carried out for a minimum of 4 h in an inert atmosphere such as Ar or  $N_2$  gas. Metal powders

such as Ti, V, Cr, Mo, etc., are typically used for the M source, but metal carbides such as TiC and Cr<sub>3</sub>C<sub>2</sub> are becoming popular to reduce impurities [19][20]. It is also reported that the metal hydrides (e.g., ZrH<sub>2</sub>) are an alternative M source to synthesize Zr<sub>2</sub>AlC or Zr<sub>3</sub>AlC<sub>2</sub>, which seems very difficult using carbides [21]. The used metal hydrides should be performed with safety measures as the evaporated H<sub>2</sub> may cause an explosion in large quantities. Al and Si are the most common A sources because of their low prices, although Ga and Ge are also used. The A elements should be added in excess of ~20 wt.% of their stoichiometric weight to compensate for the loss of thermal evaporation. As for the X elements, graphite is commonly utilized for carbide MAX with sub-stoichiometric quantities of 0.9%, and metal nitrides are the starting sources of the X elements for nitride MAX, but despite this, the nitridation of carbide MAX or mixing carbide and nitride MAX is also possible to conduct to form carbonitride MAX [22].

For the general etching process, hydrofluoric acid (HF) is the most common etchant to remove the A layer from the MAX phase. The exact etching condition depends on the type of MAX phase, HF concentration, temperature, and reaction time. Each gram of Ti<sub>3</sub>AlC<sub>2</sub> MAX can be etched at room temperature to 40 °C for 24 h, 18 h, and 5 h by adding 5, 10, and 30 wt.% HF, respectively [23]. Unlike Ti<sub>3</sub>AlC<sub>2</sub>, the V<sub>2</sub>AlC MAX type should be etched at 60 °C in 40–50 wt.% HF for 96 h for each gram, which in some cases may induce defect formation [24], although it can recently be replaced with 12 mL of 48 wt.% HF and 8 mL of 12 M HCl within 72 h at 50 °C [23]. The hazardous HF concentration should be carefully handled as it can cause burns and damage organs and tissues. An effort to eliminate or at least reduce the use of HF can be achieved with a mixture of LiF and highly concentrated HCl. Still, treating the residual F waste remains challenging to prevent its release into water resources. After this process, the produced MXenes are still in a multilayer form with an accordion-like morphology. Expanding the interlayer spacing between the 2D MXenes with intercalating compounds is needed to delaminate the multilayer structures into single-layer MXenes flakes. Several compounds have been reported to be successful in the delamination of MXenes, typically dimethyl sulfoxide (DMSO), tetrabutylammonium hydroxide (TBAOH), and tetramethylammonium hydroxide (TMAOH). These final steps produce a colloidal solution containing electrostatically stable 2D MXene flakes, which can be solution processed for further use. The lengthy steps, energy-intensive processes, and careful handling that are needed to synthesize MAX and MXenes, as explained, have been massive drawbacks for the scalable production of MXenes. Thus, more eco-friendly and sustainable techniques for producing MXenes should be future requirements and interests when one is conducting research.

## 2.2. Synthetic Strategies towards MXenes with Different Dimensionality

A comprehensive development list of MXene synthesis methods has been carried out to discover new types of MXenes and improve the functionality of the MXenes. The chemical and physical fabrication routes of MXenes could very much differ depending on the desired MXene compositions [1]. However, most of the synthesis methods of MXenes utilize a harmful chemical accessory that degenerates their functionality, notably for biomedical and environmental applications. Before discussing a more detailed strategy to obtain MXenes using green-related synthesis approaches, researchers provide an overview of the MXene synthesis methods attributed to their 0D, 1D, 2D, and 3D forms, as shown in **Figure 3**. The overview is related to the MXenes' original, derivations, and nanocomposite forms.



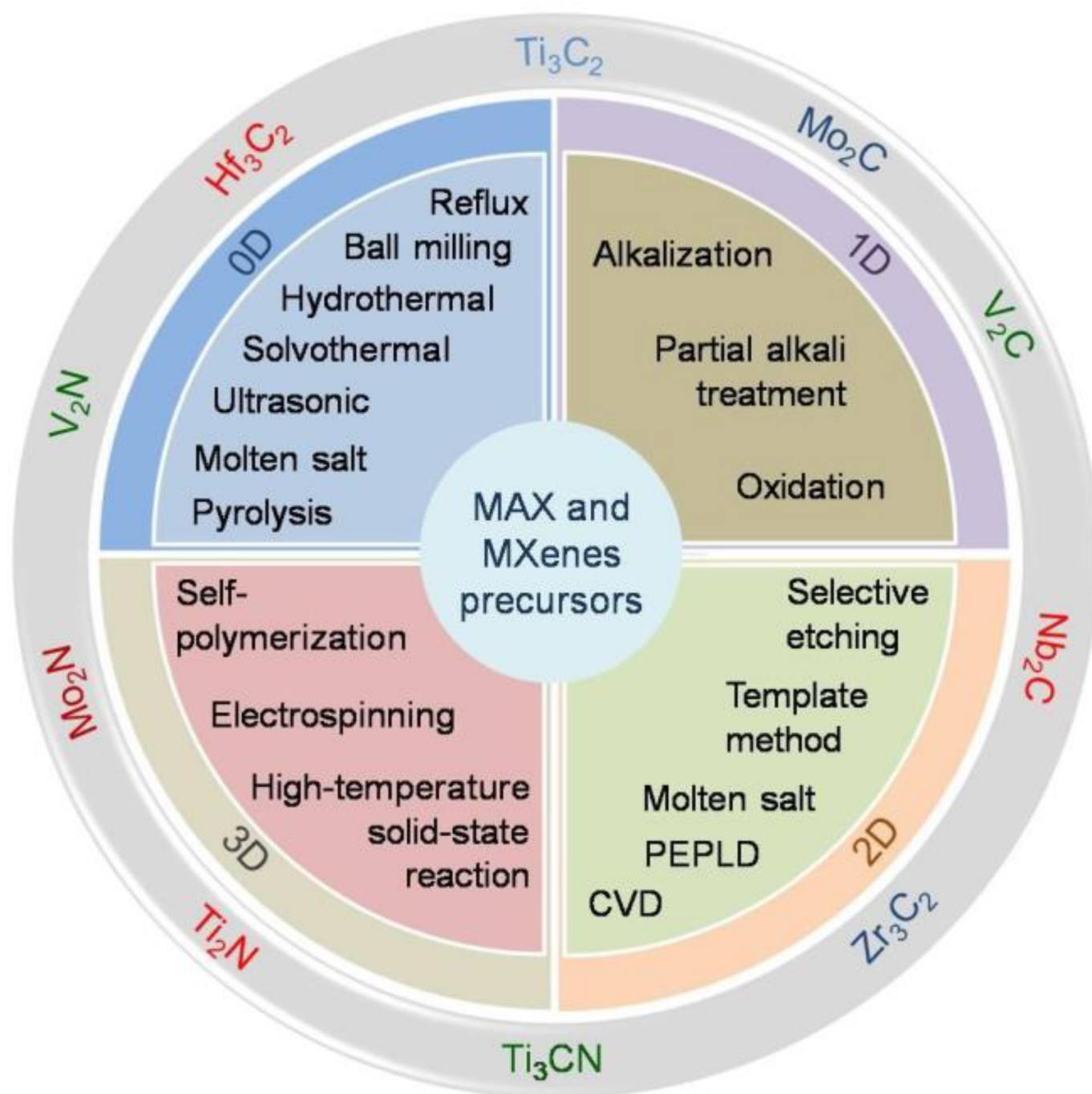


**Figure 3.** Compilation of recent fabrication methods of MXenes and derivatives depends upon their 0D, 1D, 2D, and 3D forms.

In the quantum size regime, zero-dimensional (0D) materials are usually called quantum dots (QDs). The quantum size regime is attained when the dimensions of some of the materials are smaller than their exciton Bohr radius. MXenes are among the materials that can be transformed into QDs using various synthesizing methods, including top-down and bottom-up fabrication methods. The top-down approaches mean the use of physically or chemically bonded separation or breaking larger-sized materials into smaller ones. In contrast, the bottom-up processes imply the use of physically or chemically bonded arrangements or constructing the smaller (atomic/molecule) substances

into a set of large-sized materials [25]. Only a few bottom-up methods have been successfully used to synthesize 0D MXenes, e.g., the molten salt synthesis method using molybdenum acetylacetonate, sucrose, and NaCl as parent precursors for the synthesis of the  $\text{Mo}_2\text{C}$  QDs/carbon nanosheet composite [26]. Wang et al. successfully fabricated 0D MXenes using a bottom-up approach using a pyrolysis method [27]. They used molybdic acid, zinc acetate, and 2-methylimidazole as precursors to obtain  $\text{Mo}_2\text{C}$  [27]. On the contrary, numerous top-down approaches have been conducted to obtain 0D MXenes, including liquid-phase exfoliation [28], hydrothermal [29][30], solvothermal [31], reflux or intercalation [32], ultrasonic [33][34], and ball milling methods [34][35] using 2D MXenes or directly using 3D MAX phases as the parent material.

The one-dimensional (1D) material refers to the material that is crystallized in only one direction of the crystal growth. The size expansion of the 1D materials is negligible in two dimensions, but it is not restricted in other (third) directions. One-dimensional materials could be found with several characteristics, namely nanowires, nanoribbons, nanotubes, and nanorods. Even though MXenes are categorized into 2D materials, a recent study shows they could also be formed into 1D materials. Using an alkalization process, Lian et al. successfully transformed the  $\text{Ti}_3\text{C}_2$  into 1D material [36]. They speculated that a continuous shaking treatment in an aqueous KOH solution could induce effective alkalization and delamination, essential in transforming  $\text{Ti}_3\text{C}_2$  into a nanoribbon form [36]. Using a similar method, Dong et al. fabricated  $\text{Ti}_3\text{C}_2$  MXene derivations in nanoribbons forms [37]. The two nanoribbons from  $\text{Ti}_3\text{C}_2$  were M-NTO (or  $\text{NaTiO}_{1.5}\text{O}_{8.3}$ ) and M-KTO (or  $\text{K}_2\text{Ti}_4\text{O}_9$ ), which were obtained using simultaneous oxidation and alkalization under hydrothermal conditions in NaOH and KOH solutions, respectively [37]. Nanocomposite-based 1D MXenes have also been previously reported. Using the partial alkali treatment of  $\text{Ti}_3\text{C}_2$  in an NaOH solution, the MXene derivative of the  $\text{Na}_{0.23}\text{TiO}_2$  nanobelt composed with  $\text{Ti}_3\text{C}_2$  was favorably obtained [38]. Similarly, the alkali oxidation method successfully fabricated MXenes-derived  $\text{TiO}_2$  nanowires composed of  $\text{Ti}_3\text{C}_2$  [39]. He et al. announced that they fabricated nanocomposites of a hydroxylated MXenes/carbon (h- $\text{Ti}_3\text{C}_2$ /CNTs) nanotube using an alkalization process [40].

The two-dimensional (2D) materials are the materials that are not crystallized in only one dimension as they are not restricted to grow in the other two directions; the electron and hole motion is confined in only one spatial direction, whereas free propagation is allowed to occur in two spatial directions. It is clear that MXenes are 2D materials, and they were primarily found by the use of the top-down process using selective etching of the 3D MAX phase, as previously explained in many works of literature [1]. Nonetheless, bottom-up approaches also have been developed to obtain MXenes, e.g., the molten salt technique can realize more green MXenes as it can avoid any HF-containing HF-forming chemicals [1][41]. Compared to the top-down methods, the bottom-up methods are considered more suitable for synthesizing large-area 2D materials, they can be used to grow heterostructures of 2D materials directly, and they enable the growth of atomically thin non-layered materials. Various bottom-up methods of 2D materials have been developed, and it is possible to synthesize MXenes, such as by chemical vapor deposition (CVD), the template method, and plasma-enhanced pulsed laser deposition (PEPLD) [41].

Three-dimensional (3D) materials are materials that are crystallized in three directions of growth. MXenes as 2D materials could be transformed into the 3D form when they are highly stacked in the vertical direction. Druffel et al. synthesized 3D MXenes through a high-temperature solid-state reaction that enabled the construction of 3D

crystals in high yield and purity with only fluoride ions terminating the layers [42]. Shang et al. [43] combined MXenes with rGO (graphene oxide) and facilitated the formation of a 3D structured hydrogel. As they are 2D materials, MXenes are challenging to construct in a 3D form, and it is even more difficult to do than it is for the other 2D materials because of the intrinsic properties of the MXenes [43]. Thus, MXenes are easier to transform into a 3D form when they are combined with other materials as a binder. Using electrospinning fabrication methods, Yuan et al. fabricated a flexible 3D MXene framework using a PVA/PEI mixture solution [44]. Zhang et al., on the other hand, successfully transformed a 2D  $Ti_3C_2T_x$  MXene into a 3D carbon-coated  $Ti_3C_2T_x$  architecture via the self-polymerization of dopamine over the surface of pristine 2D  $Ti_3C_2T_x$  which was achieved by a freeze-drying process and carbonization in an inert air atmosphere [45]. It was found that the self-polymerization of dopamine during the synthesis process enabled the transformation of 2D  $Ti_3C_2T_x$  into a 3D tremella-like form, and its subsequent carbonization could induce the perfect coverage of a thin carbon coating that protected the structure from air oxidation and structural aggregation [45].

## References

1. Gogotsi, Y.; Anasori, B. The Rise of MXenes. *ACS Nano* 2019, 13, 8491–8494.
2. Zamhuri, A.; Lim, G.P.; Ma, N.L.; Tee, K.S.; Soon, C.F. MXene in the lens of biomedical engineering: Synthesis, applications and future outlook. *Biomed. Eng. Online* 2021, 20, 33.
3. Naguib, M.; Mochalin, V.N.; Barsoum, M.W.; Gogotsi, Y. 25th Anniversary Article: MXenes: A New Family of Two-Dimensional Materials. *Adv. Mater.* 2014, 26, 992–1005.
4. Ijaz, I.; Gilani, E.; Nazir, A.; Bukhari, A. Detail review on chemical, physical and green synthesis, classification, characterizations and applications of nanoparticles. *Green Chem. Lett. Rev.* 2020, 13, 223–245.
5. Gour, A.; Jain, N.K. Advances in green synthesis of nanoparticles. *Artif. Cells Nanomed. Biotechnol.* 2019, 47, 844–851.
6. Jadoun, S.; Arif, R.; Jangid, N.K.; Meena, R.K. Green synthesis of nanoparticles using plant extracts: A review. *Environ. Chem. Lett.* 2021, 19, 355–374.
7. Amrillah, T. All Shapes and Phases of Nanometer-Sized Iron Oxides Made from Natural Sources and Waste Material via Green Synthesis Approach: A Review. *Cryst. Growth Des.* 2022, 22, 4640–4660.
8. Huston, M.; DeBella, M.; DiBella, M.; Gupta, A. Green Synthesis of Nanomaterials. *Nanomaterials* 2021, 11, 2130.
9. Jolly, S.; Paranthaman, M.P.; Naguib, M. Synthesis of  $Ti_3C_2T_z$  MXene from low-cost and environmentally friendly precursors. *Mater. Today Adv.* 2021, 10, 100139.

10. Luo, S.; Dong, S.; Lu, C.; Yu, C.; Ou, Y.; Luo, L.; Sun, J.; Sun, J. Rational and green synthesis of novel two-dimensional WS<sub>2</sub>/MoS<sub>2</sub> heterojunction via direct exfoliation in ethanol-water targeting advanced visible-light-responsive photocatalytic performance. *J. Colloid Interface Sci.* 2018, 513, 389–399.
11. Gupta, A.; Badruddoza, A.Z.M.; Doyle, P.S. A General Route for Nanoemulsion Synthesis Using Low-Energy Methods at Constant Temperature. *Langmuir* 2017, 33, 7118–7123.
12. Liu, K.; Zhang, J.-J.; Cheng, F.-F.; Zheng, T.-T.; Wang, C.; Zhu, J.-J. Green and facile synthesis of highly biocompatible graphene nanosheets and its application for cellular imaging and drug delivery. *J. Mater. Chem.* 2011, 21, 12034.
13. Ma, N.; Zhang, B.; Liu, J.; Zhang, P.; Li, Z.; Luan, Y. Green fabricated reduced graphene oxide: Evaluation of its application as nano-carrier for pH-sensitive drug delivery. *Int. J. Pharm.* 2015, 496, 984–992.
14. Jeon, M.; Jun, B.-M.; Kim, S.; Jang, M.; Park, C.M.; Snyder, S.A.; Yoon, Y. A review on MXene-based nanomaterials as adsorbents in aqueous solution. *Chemosphere* 2020, 261, 127781.
15. Ronchi, R.M.; Arantes, J.T.; Santos, S.F. Synthesis, structure, properties and applications of MXenes: Current status and perspectives. *Ceram. Int.* 2019, 45, 18167–18188.
16. Cheng, Y.; Zhang, Y.; Li, Y.; Dai, J.; Song, Y. Hierarchical Ni<sub>2</sub>P/Cr<sub>2</sub>CT<sub>x</sub> (MXene) composites with oxidized surface groups as efficient bifunctional electrocatalysts for overall water splitting. *J. Mater. Chem. A* 2019, 7, 9324–9334.
17. Jeitschko, W.; Nowotny, H.; Benesovsky, F. Carbides of formula T<sub>2</sub>MC. *J. Common Met.* 1964, 7, 133–138.
18. Naguib, M.; Mashtalir, O.; Carle, J.; Presser, V.; Lu, J.; Hultman, L.; Gogotsi, Y.; Barsoum, M.W. Two-Dimensional Transition Metal Carbides. *ACS Nano* 2012, 6, 1322–1331.
19. Tan, L.; Guan, C.; Tian, Y.; Dang, P.; Wang, S.; Li, J.; Li, W.; Zhao, Z. Synthesis and tribological properties of ultrafine Cr<sub>2</sub>AlC MAX phase. *J. Ceram. Soc. Jpn.* 2019, 127, 754–760.
20. Shalini Reghunath, B.; Davis, D.; Sunaja Devi, K.R. Synthesis and characterization of Cr<sub>2</sub>AlC MAX phase for photocatalytic applications. *Chemosphere* 2021, 283, 131281.
21. Tunca, B.; Lapauw, T.; Karakulina, O.M.; Batuk, M.; Cabioc'h, T.; Hadermann, J.; Delville, R.; Lambrinou, K.; Vleugels, J. Synthesis of MAX Phases in the Zr-Ti-Al-C System. *Inorg. Chem.* 2017, 56, 3489–3498.
22. Du, Z.; Wu, C.; Chen, Y.; Zhu, Q.; Cui, Y.; Wang, H.; Zhang, Y.; Chen, X.; Shang, J.; Li, B.; et al. High-Entropy Carbonitride MAX Phases and Their Derivative MXenes. *Adv. Energy Mater.* 2022, 12, 2103228.

23. Alhabeb, M.; Maleski, K.; Anasori, B.; Lelyukh, P.; Clark, L.; Sin, S.; Gogotsi, Y. Guidelines for Synthesis and Processing of Two-Dimensional Titanium Carbide (Ti<sub>3</sub>C<sub>2</sub>T<sub>x</sub> MXene). *Chem. Mater.* 2017, 29, 7633–7644.
24. Sang, X.; Xie, Y.; Lin, M.-W.; Alhabeb, M.; Van Aken, K.L.; Gogotsi, Y.; Kent, P.R.C.; Xiao, K.; Unocic, R.R. Atomic Defects in Monolayer Titanium Carbide (Ti<sub>3</sub>C<sub>2</sub>T<sub>x</sub>) MXene. *ACS Nano* 2016, 10, 9193–9200.
25. Tian, L.; Li, Z.; Wang, P.; Zhai, X.; Wang, X.; Li, T. Carbon quantum dots for advanced electrocatalysis. *J. Energy Chem.* 2021, 55, 279–294.
26. Cheng, H.; Ding, L.-X.; Chen, G.-F.; Zhang, L.; Xue, J.; Wang, H. Molybdenum Carbide Nanodots Enable Efficient Electrocatalytic Nitrogen Fixation under Ambient Conditions. *Adv. Mater.* 2018, 30, 1803694.
27. Wang, Y.; Li, C.; Han, X.; Liu, D.; Zhao, H.; Li, Z.; Xu, P.; Du, Y. Ultrasmall Mo<sub>2</sub>C Nanoparticle-Decorated Carbon Polyhedrons for Enhanced Microwave Absorption. *ACS Appl. Nano Mater.* 2018, 1, 5366–5376.
28. Xu, N.; Li, H.; Gan, Y.; Chen, H.; Li, W.; Zhang, F.; Jiang, X.; Shi, Y.; Liu, J.; Wen, Q.; et al. Zero-Dimensional MXene-Based Optical Devices for Ultrafast and Ultranarrow Photonics Applications. *Adv. Sci.* 2020, 7, 2002209.
29. Rafieerad, A.; Yan, W.; Amiri, A.; Dhingra, S. Bioactive and trackable MXene quantum dots for subcellular nanomedicine applications. *Mater. Des.* 2020, 196, 109091.
30. Xu, Q.; Ma, J.; Khan, W.; Zeng, X.; Li, N.; Cao, Y.; Zhao, X.; Xu, M. Highly green fluorescent Nb<sub>2</sub>C MXene quantum dots. *Chem. Commun.* 2020, 56, 6648–6651.
31. Feng, Y.; Zhou, F.; Deng, Q.; Peng, C. Solvothermal synthesis of in situ nitrogen-doped Ti<sub>3</sub>C<sub>2</sub> MXene fluorescent quantum dots for selective Cu<sup>2+</sup> detection. *Ceram. Int.* 2020, 46, 8320–8327.
32. Qin, Y.; Wang, Z.; Liu, N.; Sun, Y.; Han, D.; Liu, Y.; Niu, L.; Kang, Z. High-yield fabrication of Ti<sub>3</sub>C<sub>2</sub>T<sub>x</sub> MXene quantum dots and their electrochemiluminescence behavior. *Nanoscale* 2018, 10, 14000–14004.
33. Yu, X.; Cai, X.; Cui, H.; Lee, S.-W.; Yu, X.-F.; Liu, B. Fluorine-free preparation of titanium carbide MXene quantum dots with high near-infrared photothermal performances for cancer therapy. *Nanoscale* 2017, 9, 17859–17864.
34. Pandey, P.; Sengupta, A.; Parmar, S.; Bansode, U.; Gosavi, S.; Swarnkar, A.; Muduli, S.; Mohite, A.D.; Ogale, S. CsPbBr<sub>3</sub>–Ti<sub>3</sub>C<sub>2</sub>T<sub>x</sub> MXene QD/QD Heterojunction: Photoluminescence Quenching, Charge Transfer, and Cd Ion Sensing Application. *ACS Appl. Nano Mater.* 2020, 3, 3305–3314.



35. Xu, Q.; Ding, L.; Wen, Y.; Yang, W.; Zhou, H.; Chen, X.; Street, J.; Zhou, A.; Ong, W.-J.; Li, N. High photoluminescence quantum yield of 18.7% by using nitrogen-doped Ti<sub>3</sub>C<sub>2</sub> MXene quantum dots. *J. Mater. Chem. C* 2018, 6, 6360–6369.
36. Lian, P.; Dong, Y.; Wu, Z.-S.; Zheng, S.; Wang, X.; Sen, W.; Sun, C.; Qin, J.; Shi, X.; Bao, X. Alkalized Ti<sub>3</sub>C<sub>2</sub> MXene nanoribbons with expanded interlayer spacing for high-capacity sodium and potassium ion batteries. *Nano Energy* 2017, 40, 1–8.
37. Dong, Y.; Wu, Z.-S.; Zheng, S.; Wang, X.; Qin, J.; Wang, S.; Shi, X.; Bao, X. Ti<sub>3</sub>C<sub>2</sub> MXene-Derived Sodium/Potassium Titanate Nanoribbons for High-Performance Sodium/Potassium Ion Batteries with Enhanced Capacities. *ACS Nano* 2017, 11, 4792–4800.
38. Huang, J.; Meng, R.; Zu, L.; Wang, Z.; Feng, N.; Yang, Z.; Yu, Y.; Yang, J. Sandwich-like Na<sub>0.23</sub>TiO<sub>2</sub> nanobelt/Ti<sub>3</sub>C<sub>2</sub> MXene composites from a scalable in situ transformation reaction for long-life high-rate lithium/sodium-ion batteries. *Nano Energy* 2018, 46, 20–28.
39. Li, N.; Jiang, Y.; Zhou, C.; Xiao, Y.; Meng, B.; Wang, Z.; Huang, D.; Xing, C.; Peng, Z. High-Performance Humidity Sensor Based on Urchin-Like Composite of Ti<sub>3</sub>C<sub>2</sub> MXene-Derived TiO<sub>2</sub> Nanowires. *ACS Appl. Mater. Interfaces* 2019, 11, 38116–38125.
40. He, X.; Jin, S.; Miao, L.; Cai, Y.; Hou, Y.; Li, H.; Zhang, K.; Yan, Z.; Chen, J. A 3D Hydroxylated MXene/Carbon Nanotubes Composite as a Scaffold for Dendrite-Free Sodium-Metal Electrodes. *Angew. Chem. Int. Ed.* 2020, 59, 16705–16711.
41. Xu, C.; Chen, L.; Liu, Z.; Cheng, H.-M.; Ren, W. Bottom-Up Synthesis of 2D Transition Metal Carbides and Nitrides. In *2D Metal Carbides and Nitrides (MXenes)*; Anasori, B., Gogotsi, Y., Eds.; Springer International Publishing: Cham, Switzerland, 2019; pp. 89–109. ISBN 978-3-030-19025-5.
42. Druffel, D.L.; Lanetti, M.G.; Sundberg, J.D.; Pawlik, J.T.; Stark, M.S.; Donley, C.L.; McRae, L.M.; Scott, K.M.; Warren, S.C. Synthesis and Electronic Structure of a 3D Crystalline Stack of MXene-Like Sheets. *Chem. Mater.* 2019, 31, 9788–9796.
43. Shang, T.; Lin, Z.; Qi, C.; Liu, X.; Li, P.; Tao, Y.; Wu, Z.; Li, D.; Simon, P.; Yang, Q. 3D Macroscopic Architectures from Self-Assembled MXene Hydrogels. *Adv. Funct. Mater.* 2019, 29, 1903960.
44. Yuan, W.; Yang, K.; Peng, H.; Li, F.; Yin, F. A flexible VOCs sensor based on a 3D Mxene framework with a high sensing performance. *J. Mater. Chem. A* 2018, 6, 18116–18124.
45. Zhang, P.; Soomro, R.A.; Guan, Z.; Sun, N.; Xu, B. 3D carbon-coated MXene architectures with high and ultrafast lithium/sodium-ion storage. *Energy Storage Mater.* 2020, 29, 163–171.

Retrieved from <https://encyclopedia.pub/entry/history/show/90403>